

LATTICE AND OPTICS DESIGNS OF THE TEST ERL IN JAPAN

K. Harada, T. Kasuga, Y. Kobayashi, T. Miyajima, T. Ozaki, S. Sakanaka, K. Satoh, M. Tobiya
High Energy Accelerator Research Organization (KEK), Oho, Tsukuba, Ibaraki 305-0801, Japan

R. Hajima, ERL Development Group, Japan Atomic Energy Agency (JAEA),
Tokai, Naka, Ibaraki 319-1195, Japan

N. Nakamura, H. Takaki, Institute for Solid State Physics (ISSP), University of Tokyo,
5-1-5 Kashiwanoha, Kashiwa, Chiba 277-8581, Japan

M. Shimada, UVSOR, Institute for Molecular Science,
National Institutes of Natural Sciences, Myodaiji-cho, Okazaki, Aichi 444-8585, Japan

Abstract

To open up unexploited fields in the synchrotron radiation research, a new synchrotron light source based on the energy recovery linac (ERL) is under contemplation by the Japanese ERL collaboration. To clarify both physical and technological challenges for this project, a test ERL is planned to be built at a KEK campus. This paper presents current lattice design of the test ERL, and discusses single-particle optics issues under beam recirculation and under bunch compression.

INTRODUCTION

A new synchrotron light source based on the ERL is under contemplation [1,2] by the Japanese ERL collaboration, which is organized by researchers of KEK, JAEA, ISSP, UVSOR, and SPring-8. This plan is aimed at recirculating 5-GeV, ultra-low emittance beams of 10-100 pm-rad at high beam currents of 100 mA, as well as producing short-pulse X-rays having sub-picoseconds lengths. Before constructing such a facility, we should establish basic technologies needed, and must demonstrate them in a small test facility. We plan to construct the test ERL for this purpose.

The test ERL is aimed at demonstrating such operations as: (1) recirculating high current beams of 10-100 mA, (2) production, acceleration, and transportation of ultra-low emittance beams, (3) bunch compression down to r.m.s. lengths of about 0.1 ps, and (4) accommodating user's demo experiments. A current plan comprises a DC photocathode gun, a 5-MeV superconducting injector,

a 60-200 MeV main linac, and a recirculating loop. The goals of the test ERL are shown in Table 1. R&D on the key technologies, such as a low-emittance DC photocathode gun [3] and superconducting cavities [4], are on the way.

In this paper, we present a lattice design and discuss single-particle optics issues concerning the recirculating loop of the test ERL. Effects of the coherent synchrotron radiation (CSR) are discussed in an accompanying paper [5].

Table 1: Principal parameters of the planned test ERL.

Injection energy	5 MeV
Maximum energy	60-200 MeV
Normalized emittance	1-0.1 mm-mrad
Beam current	10-100 mA
rf frequency	1.3 GHz

LATTICE DESIGN

The present lattice of the test ERL (see Fig. 1) comprises two 180° arcs and two long straight sections. A triple-bend-achromat (TBA) lattice is adopted for the arcs, since it allows us to adjust R_{56} easily and that it is a candidate lattice for the future ERL. One of the straight sections can accommodate two cryomodules, a merger, and an extractor. We currently suppose to house four nine-cell cavities in a cryomodule. The other straight section can accommodate a chicane for circumference tuning and an undulator for evaluating the beam quality.

BEAM OPTICS

Optimizations of linear and higher-order optics are very important to keep the beam quality along the recirculating loop. In addition, under a commissioning stage of the test ERL, possible timing jitters, or other errors, can cause relatively large momentum deviations of the beams. Therefore, wide momentum acceptance will be essential for its successful commissioning. It is also important for effective bunch compression down to sub picoseconds.

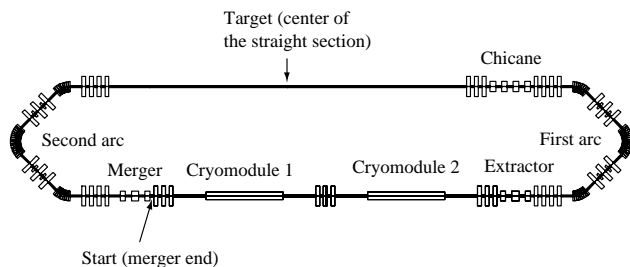


Figure 1: Lattice of the test ERL. In the simulations, particles start from the exit of the merger. The target location for the optimizations is the center of the straight section.

Nonlinear Optics Distortions for Off-momentum Particles

The trajectory of particles is a superposition of the central orbit and the betatron oscillations. Without any lattice errors, the coordinates of the central orbit for an off-momentum particle (momentum deviation: $\delta = \Delta P/P$) are given by

$$\Delta x = R_{16}\delta + T_{166}\delta^2 + U_{1666}\delta^3 + \dots, \quad (1a)$$

$$\Delta x' = R_{26}\delta + T_{266}\delta^2 + U_{2666}\delta^3 + \dots, \quad (1b)$$

$$\Delta z = R_{56}\delta + T_{566}\delta^2 + U_{5666}\delta^3 + \dots, \quad (1c)$$

where Δx and $\Delta x'$ are the horizontal displacement and the divergence at a target position, respectively, and Δz is the deviation of the path length from that of the reference particle. The first order terms can be written by

$$R_{16} = \eta, \quad R_{26} = \eta', \quad \text{and} \quad R_{56} = \int_{\text{Bend}} \frac{\eta}{\rho} ds, \quad (2)$$

where η and η' are the horizontal dispersion and its slope, respectively, and ρ is the bending radius.

In the straight sections where rf cavities and a test undulator will be installed, we required the achromatic conditions, $R_{16} = 0$ and $R_{26} = 0$. We also required the isochronous condition, $R_{56} = 0$, for beam recirculation without bunch compression. These conditions were achieved by adjusting the strengths of the quadrupole magnets in the arc section.

Next, we considered preserving the low projected emittance at an exit of the first arc section when the momentum spread of the beam was relatively large. In the horizontal direction, higher-order distortions of the dispersion function affected the growth of the projected emittance and the bunch length. Corrections of the second order dispersions (T_{166} , T_{266} , and T_{566}) using the sextupole magnets with two kinds of strength located in the arc section were effective to preserve the projected emittance and the bunch length.

In the vertical direction, although the distortions of betatron oscillations for off-momentum particles were not so large, we corrected the chromatic distortions of the betatron functions.

Corrections of Higher-Order Dispersion by Sextupoles

The above sextupole correction was carried out in a simplified lattice without having any cavities, as shown in Fig. 2. The optical functions for off-momentum particles were distorted without the sextupole correction, as shown in Fig. 3(a). Especially, the distortion of the dispersion function resulted in the orbit distortion for the off-momentum particles, and then the horizontal projected emittance and the bunch length enlarged. When the conditions such as $T_{166} = 0$, $T_{266} = 0$, and $T_{566} = 0$ were realized using the sextupoles magnets, the distortion of the dispersion function became small, as shown in Fig. 3(b).

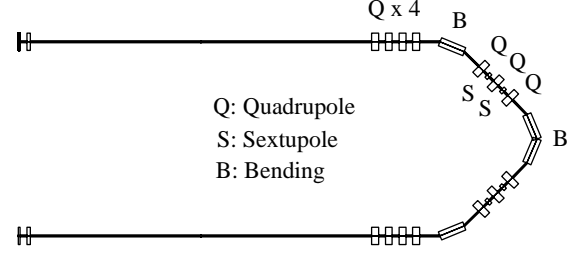


Figure 2: Simplified lattice used for the chromaticity corrections. A half of the test ERL lattice was used where nothing is inserted in the long straight section.

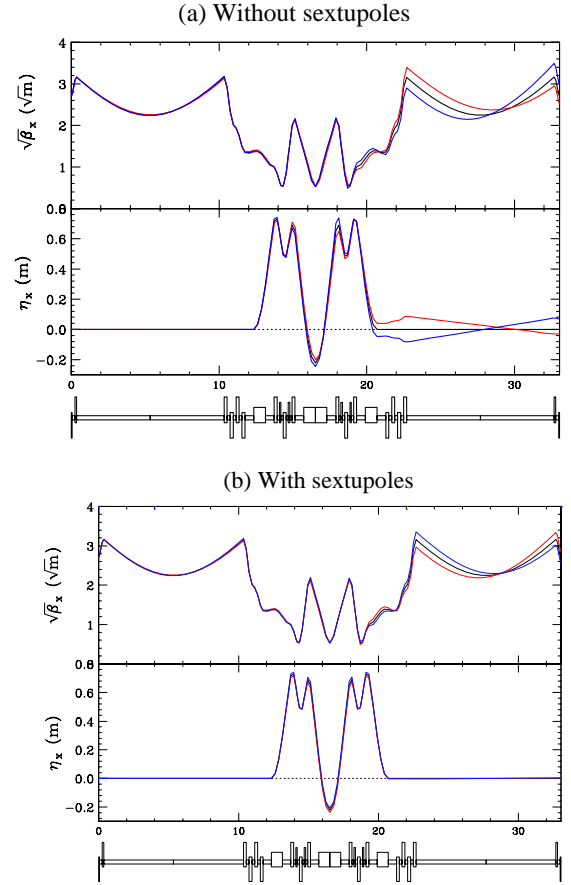


Figure 3: Optical functions for off-momentum particles. The black traces indicate the optical functions for on-momentum particles, while the red and the blue traces indicate those for the off-momentum particles with the momentum deviations of +1% and -1%, respectively. (a) Without any corrections, and (b) with sextupole correction.

Figure 4 shows the deviations of the coordinates as a function of the initial momentum deviation. Due to the sextupole correction, the deviations became drastically small in the range from -0.03% to 0.03%. These terms (T_{166} , T_{266} , and T_{566}) affected the particle motions very strongly, and then resulted in forming beam halos or losing the particles with large momentum deviations. Therefore, we think that the sextupole correction is very important to reduce the particle losses.

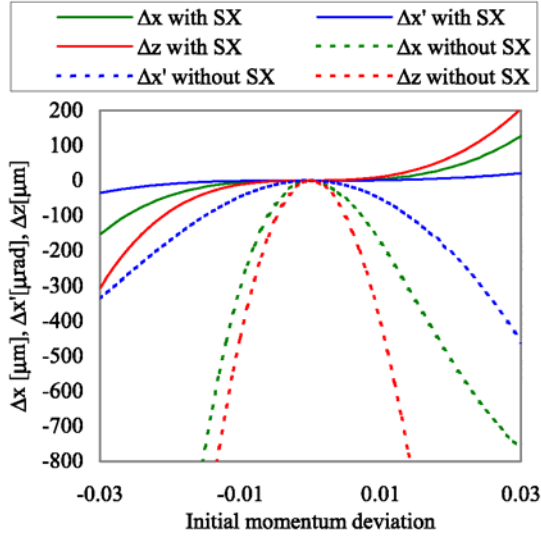


Figure 4: Coordinates (Δx , $\Delta x'$, and Δz) of the central orbit at the end of the half recirculation path. Solid and dashed lines indicate those coordinates with and without sextupole corrections, respectively.

TRACKING SIMULATIONS

We examined the particle motions using multi-particle tracking simulations under two operation modes: one is the mode of a simple beam recirculation and the other is the mode of bunch compression. The tracking simulations were conducted from the exit of the merger to the center of the straight section where is a target point. Initial beam parameters at the exit of the merger were assumed to be the normalized emittance of 1 mm-mrad, the r.m.s. energy spread of 1×10^{-4} , the r.m.s. bunch length of 1 ps, and the initial momentum of 5 MeV/c, respectively. At the moment, no effects of CSR were included.

Beam Recirculation

For the simple beam recirculation, the beam was accelerated at the on-crest of the rf in the accelerating section and the momentum reached to about 165 MeV/c. The optical functions are shown by the red lines in Fig. 5. The isochronous condition ($R_{56} = 0$) was set at the arc section. The results are shown in Figs. 6. The momentum spread was mainly determined by the rf curvature, and it was calculated to be only about 6×10^{-5} in r.m.s. Since the momentum spread was preserved to be a small value, the growths of both the projected emittance and the bunch length were not observed. The r.m.s. beam sizes calculated by the tracking simulation in this mode agreed well with those obtained using the Twiss parameters.

Bunch Compression

Next, we considered compressing the bunch length using a magnetic compression method, which is realized by the accelerating section and the first arc section. As an example, we chose the acceleration phase of 70 degrees

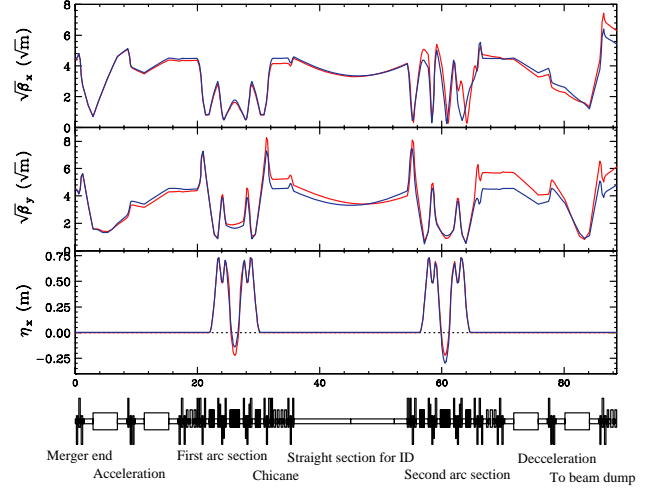


Figure 5: Optical functions of the test ERL for the beam recirculation (red lines) and for the bunch compression (blue lines), respectively. For both operations, the initial Twiss parameters were chosen to be $\beta_x = \beta_y = 10$ m, $\alpha_x = \alpha_y = 0$, $\eta_x = 0$, and $\eta'_x = 0$, respectively.

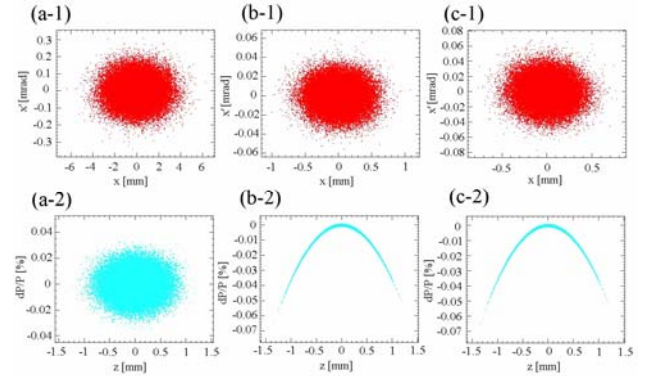


Figure 6: Results of the tracking simulation for the beam recirculation. (a) Initial beam distribution at 5 MeV/c, (b) after the acceleration to 165 MeV/c, and (c) at the center of the straight section. The upper figures show the particle distribution in the horizontal phase space (x , x'), while the lower figures show the longitudinal phase space (z , $\Delta P/P$).

(i.e., off-crest by 20 degrees) in the accelerating section. Though the phase was relatively large, it was convenient to investigate the behaviors of particles with large momentum deviations while the final momentum was limited to be about 155 MeV/c.

In order to compress and decompress the bunch length using the arc sections, we controlled the strength of the quadrupoles to be $R_{56} = +0.11$ m at the first arc section, and -0.11 m at the second arc section. The results of the beam tracking, conducted under these conditions of the bunch compression, are shown in Fig. 7. As shown in Fig. 7(c-2), the bunch was compressed to be 0.17 ps r.m.s. without sextupole corrections, but Δz showed a parabolic dependence on δ (red points in Fig. 7(c-2)). While the r.m.s. momentum spread after the acceleration was about 0.3%, the momentum deviation of the particles at the tail of the bunch reached to about 1.5%, as shown in the Fig. 7(b-2). Without sextupole corrections, the horizontal

orbits of the particles with large momentum deviations were distorted due to the higher-order dispersion. As a result, the beam distribution was largely deformed from its initial distribution, and then, the large beam tail was formed, as indicated by the red points in Fig. 7(c-1). Thus, we needed to correct the higher-order dispersion for reducing the beam tail. This correction was carried out by the sextupole magnets with two kinds of strength (two family sextupoles) located in the arc sections.

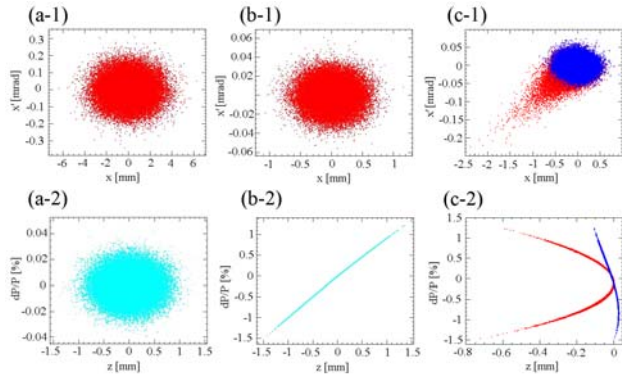


Figure 7: Results of the tracking simulation for the bunch compression. (a) Initial beam distribution at 5 MeV/c, (b) after the acceleration to 155 MeV/c, and (c) at the center of the straight section. The upper figures indicate the particle distribution in the horizontal phase space (x, x'), while the lower figures indicate the longitudinal phase space ($z, \Delta P/P$). In the figures (c-1) and (c-2), the blue and the red points indicate the cases with and without the sextupole correction, respectively.

In order to optimize the sextupole correction, the beam distributions at the target position were calculated for many combinations, (K_2^1, K_2^2), of the strengths of two family sextupoles in the range from -20 m^{-2} to $+20 \text{ m}^{-2}$. As a result, we adopted the sextupole strengths (K_2^1, K_2^2) = (6, 9), which could achieve the shortest bunch length without the growth of the horizontal projected emittance. The higher-order dispersions were calculated to be $T_{166} = 0$, $T_{266} = 0$ and $T_{566} = 0.64 \text{ m}$ for the arc section with this set. Due to the correction of the higher-order dispersion, the stability of the transverse motion was improved for the off-momentum particles, and the beam tail was reduced drastically. The effect of the rf curvature on the bunch length was also cancelled by the T_{566} at the arc section, and then, much shorter bunch length of 0.07 ps r.m.s. could be obtained in this calculation.

In the vertical direction, the projected emittance was preserved well even without sextupole corrections, and the beam sizes agreed well with those of the analytical calculation using the Twiss parameters. The sextupole correction for the higher-order dispersions in the horizontal direction allowed us to preserve the emittance in the vertical direction.

CONCLUSIONS

The lattice design of the test ERL was presented, and its single-particle optics issues were discussed. To obtain a wide momentum aperture of the recirculating loop, as well as to preserve low projected emittances, the chromaticity corrections were examined carefully. We presented optimized chromatic corrections both for the simple beam recirculation and for the bunch compression.

ACKNOWLEDGMENT

The authors would like to thank the members of the Japanese ERL collaboration for useful discussions.

REFERENCES

- [1] T. Kasuga *et al.*, APAC07, TUPMA046.
- [2] T. Kasuga *et al.*, “Status of R&D Efforts Toward the ERL-based Future Light Source in Japan”, to be presented at PAC07.
- [3] N. Nishimori, R. Hajima, H. Iijima, R. Nagai, and T. Nishitani, “Development of an electron gun for the ERL light source in Japan”, in these proceedings.
- [4] H. Sakai *et al.*, “Development of a 1.3GHz superconducting cavity for the ERL main linac in Japan”, in these proceedings.
- [5] M. Shimada, K. Harada, and R. Hajima, “Bunch compression and the emittance growth due to CSR”, in these proceedings.